Surface Characterization and Adsorption studies of Bambusa vulgaris-a low cost adsorbent

Daniel Kibami [1, 2*], Chubaakum Pongener [1,] K.S. Rao[1], Dipak sinha[1]

[1]*Department of Chemistry, Nagaland University, Lumami-798627, Nagaland, India*
[2]*Department of Chemistry, Fazl Ali College, Mokokchung-789601, Nagaland, India*

Abstract

The raw materials for the synthesis of Activated carbon were taken from the stem and leaves of the plant *Bambusa vulgaris.* The raw materials were given thermal treatment which was subsequently followed by chemical activation using 0.1N HNO_3 and 0.1N H_3PO_4. The parameters included in the surface characterization of activated carbons consist of FTIR, EDX, SEM and surface area by BET (method). Activated carbon provides a large surface area with well developed pores. Adsorption studies of Methylene blue on the activated carbon were studied for removal of dye from water.

1. Introduction

Activated carbons are known for their large surface area, microporous structure, high adsorption capacity, and high degree of surface reactivity. Depending on the functional group and ions present on the surface of the activated carbon, its adsorption quality varies [1-3]. Some of their important applications are the adsorptive removal of color, and other undesirable organic and inorganic pollutants from drinking water, in the treatment of industrial waste water. [2,3]. Activated carbon is obtained from a carefully controlled process of dehydration, carbonization and oxidation of organic substances [4,5]. It can be prepared for research in the laboratory from a large number of materials. However, the most commonly used ones in commercial practice primarily industrial and agricultural byproducts and forest wastes, such as coconut shell [6], sugar beet bagasse [7], rice husk [8], bamboo [9], rattan sawdust [10], molasses [11], rubber wood sawdust [12], oil palm fiber [13], waste apricot [14], and coconut husk [15].

Carbonization is a heat treatment at 400-800 °C which converts raw materials to carbon by minimizing the content of volatile matter and increasing the carbon content of the material. This increases the materials strength and creates an initial porous structure which is necessary if the carbon is to be activated. Adjusting the conditions of carbonization can affect the final product significantly. An increased carbonization temperature increases reactivity, but at the same time decreases the volume of pores present. This decreased volume of pores is due to an increase in the condensation of the material at higher temperatures of carbonization which yields an increase in mechanical strength. Therefore, it becomes important to choose the correct process temperature based on the desired product of carbonization [1]. After the initial porous structure has been created by carbonization, this pore structure in carbonized char is further developed and enhanced during the activated carbon process, which converts the carbonized raw material into a form that contains the greatest possible number of randomly distributed pores of various sizes and shapes, producing an extended and extremely high surface area of the product [5]. Activation can be carried out by chemical activation. The objective of this study is to produce activated carbon from locally available biowaste with two different acids, characterization of the produced activated carbons and finally examine the changes in the adsorption capacity towards transition metal ions by the formation of various oxygen and nitrogen surface functionalities by oxidation of activated carbons of similar porosity with nitric acid and phosphoric acid.

2. Materials and methods

2.1 Preparation of activated carbon

Activated carbon in powder form is prepared by the pyrolysis of Bambusa vulgaris (BVC). Stem and leaves of BVC were collected, washed, dried, and crushed before carbonizing in a uniform nitrogen flow in a horizontal

tube furnace electrically heated at 600 ^{o}C for 4 hours. Then the activated carbon was cooled to room and ground to 45μm mesh. These powdered carbons were subjected to liquid phase oxidation with 0.1N HNO_3 and 0.1 N H_3PO_4. After that the carbons were washed with double-distilled water to remove the excess acid and dried at 150°C for 12hours. All the activated carbons (BVC) are chemically activated with 0.1N solution HNO_3 and H_3PO_4. The powdered activated carbon obtained after HNO_3 and H_3PO_4 treatment has a particle size in the range of 40-50 μm mesh.

3. Surface characterization of prepared carbons

3.1 Determination of surface area (BET method)

BET-N_2 adsorption experiments were carried out manometrically using an Autosorb (Quanta Chrome Crop). Prior to gas adsorption measurements, the carbon samples were degassed at 200°C in a vacuum condition for a period of at least 24 h. Nitrogen adsorption isotherms were measured at a series of different pressures at -196°C. And the BET surface area was determined by means of the standard BET equation.

$$\frac{P}{V(P-P_0)} = \frac{1}{V_m-C} + \frac{C-1}{V_m C}\frac{P}{P_0}$$

(1)

The surface area is determined by the following equation

$$S_{BET} = \frac{N_A A_M V_m 10^{-20}}{m_s V_M}$$

(2)

Where;

S_{BET} is the BET surface area (m^2 /g)

N_A is Avogadro's number (6.023 x 10^{23} molecules/mole)

A_M is the area occupied by an adsorbate molecule (16.2 Å^2 for nitrogen)

V_m The quantity of gas adsorbed for monolayer coverage of surface (cm^3)

m_s is the mass of the solid analyzed (g)

V_M is the molar volume of gas (22,414 cm^3/mol)

For nitrogen as adsorptive gas, equation (2) becomes

$$S_{BET} = \frac{4.35 V_m}{m_s}$$

3.2 Determination of zero point charge (pH ZPC)

pH_{zpc} of an adsorbent is important because it indicates the net surface charge of the carbon in solution[16,17]. The pH_{zpc} is the point where the curve of pH (final) vs pH (initial) intersects the line pH (initial) = pH (final). In order to determine the pH of point of zero charge 0.1g of activated carbons is added to 200ml solution of 0.1M NaCl whose initial pH has been measured and adjusted with NaOH or HCl. The containers were sealed and placed on a shaker for 24hrs after which the pH was measured (see table 1 & 2).

Table 1: Determination of initial pH and final pH of BVC (HNO_3)

Sl.No	pH$_i$	pH$_f$	pH$_{f-i}$
1	7.036	7.28	0.244
2	7.14	7.352	0.212
3	7.338	7.481	0.143
4	7.469	7.55	0.081
5	7.54	7.572	0.032
6	7.66	7.596	-0.064
7	7.864	7.748	-0.116
8	8.004	7.838	-0.166
9	8.186	7.939	-0.247
10	8.302	7.974	-0.328
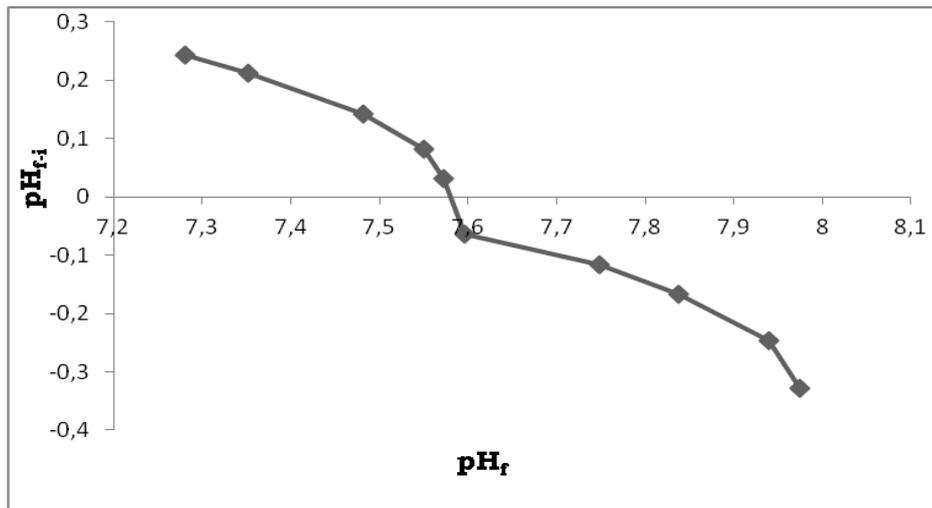
Fig 1: Plot of pH_f vs $pH_{f\text{-}I}$ of BVC (HNO$_3$)

Table 2: Determination of initial pH and final pH of BVC (H$_3$PO$_4$)

Sl.No.	pH_i	pH_f	$pH_{f\text{-}i}$
1	7.01	7.19	0.18
2	7.11	7.24	0.13
3	7.39	7.49	0.1
4	7.62	7.68	0.06
5	7.68	7.72	0.04
6	7.77	7.75	-0.02
7	7.97	7.921	-0.049
8	8.03	7.935	-0.095
9	8.16	7.974	-0.186
10	8.24	7.989	-0.251
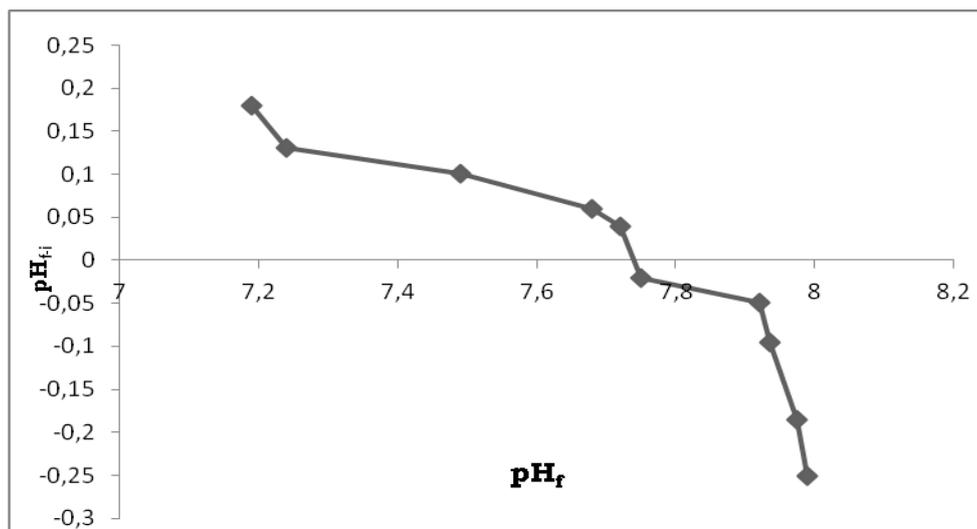
Fig 2: Plot of pH_f vs $pH_{f\text{-}i}$ of BVC (H$_3$PO$_4$)

3.3 Iodine number

Iodine number is the mass (mg) of iodine adsorbed from a standard 0.1 N (0.05 M) iodine solutions, when the equilibrium iodine concentration is exactly 0.02 N (0.01 M). According to the procedure defined by ASTM D4607 - 94(2006) [18], for determination of iodine number 0.7- 2 g of activated carbon was added with 10ml of 5% HCl and swirled in a conical flask until the entire activated carbon was wetted. The wetted solution was then

boiled for exactly 30 seconds and the solution was cooled to room temperature. Then 100ml of 0.1N iodine solution was added to the contents of the conical flask. This solution was filtered using a Whatman 2V filter paper. Later 50ml of this filtrate was then titrated against 0.10 N sodium thiosulphate until the yellow colour had almost disappeared. 1 ml starch indicator was added and the titration was continued until the blue colour just disappears. The equilibrium concentration is determined by calculation using the amount of sodium thiosulphate used in the titration. If this equilibrium concentration was not within the range of 0.008 to 0.334, then the procedure was repeated with a different amount of activated carbon.

Calculation of iodine number :

X/M = A-(DF x B x S)/ M

Where   X/M = iodine number (mg/g)
$A = 12693N_2$, $B = 126.93N_1$, $C = N_1/ (50 \times S)$, C = residual iodine (N),
S = sodium thiosulfate (ml), M = carbon used (g),
N_1 = Concentration of sodium sulphate (N)
N_2= Concentration of iodine (N)
DF = dilution factor = (I + H)/F
I = Initial iodine, H = 5% Hydrochloric acid (ml), F = filtrate (ml)

3.4 Boehm's Titration
The presence of surface functional groups in the activated carbons was quantified by Boehm titration method [19, 20]. About 1.0 g of activated carbon was mixed with each of 50 ml solution (0.1 M) of NaOH, $NaHCO_3$ and Na_2CO_3 respectively, for 24 hours with continuous stirring. Then, the solid phase was separated from the aqueous solution by vacuum filtration. 10 ml of each filtrate was used for the excess acid titration by 0.1 M HCl (hydrochloric acid). The phenolic group content on the carbon surface was determined as the amount of 0.1 M $NaHCO_3$ consumed by the sample. Lactonic group content was calculated as the difference between the amounts of 0.1 M Na_2CO_3 and 0.1 M $NaHCO_3$ consumed by the activated carbon sample. Carboxylic group is obtained by subtracting the amount of 0.1 M Na_2CO_3 consumed by the activated carbon from the amount of 0.1 M NaOH consumed. This method was used to calculate the concentration of acid groups on activated carbon surface under the following assumptions. Sodium hydroxide (NaOH) neutralizes carboxylic, phenolic and lactonic groups. Sodium carbonate (Na_2CO_3) neutralizes only carboxylic and phenolic groups. Sodium bicarbonate ($NaHCO_3$) only neutralizes carboxylic groups (table.3).

Table 3: Surface properties of *Bambusa vulgaris*

Properties	B.V.C(HNO_3)	B.V.C(H_3PO_4)
Surface area m^2/g (BET method)	570	530
Phzpc	7.58	7.71
Iodine number(mg/g)	976.19	846.03
Surface acid groups (meq/g)		
I Carboxylic	1.60	1.45
II Lactonic	0.30	0.07
III Phenolic	0.20	0.41
Total basic groups (meq/g)	3.91	3.42

3.5 Fourier transform infra-red spectroscopy
The spectra were recorded using Perkin–Elmer SPECTRUM-2000 spectrometer. Carbon samples were dried in a drier, then 2 mg of each sample was powdered and mixed with 300 mg of anhydrous KBr (Merck; for spectroscopy). The mixture was pressed under vacuum to obtain the pellets. The spectra were performed between 4000 and 400 cm^{-1} (100 scans). The background spectrum of air was subtracted from the spectra of the samples. The carbon samples were investigated using this technique (fig.3 and fig.4).

Table 4: FTIR spectrum band assignments

Wave number (cm^{-1})		Assignment
BVC(HNO$_3$)	BVC(H$_3$PO$_4$)	
3125	3215	O-H stretching in hydrogen bond.
----	2714	Alkane (C-H Stretching)
2187	2142,2071	C≡C (stretching)
1687	1821,1678,1642	C=O in carboxylic, aldehydes, ketones, esters and lactones
1510	--	C=C in aromatics or C=O stretch
----	1447	C-H deformation in alkane
1125	1245	C-O stretch in phenols, ethers, lactones
1062	1068	Alcoholic C-O stretch
687,625	874,724	Plane deformation
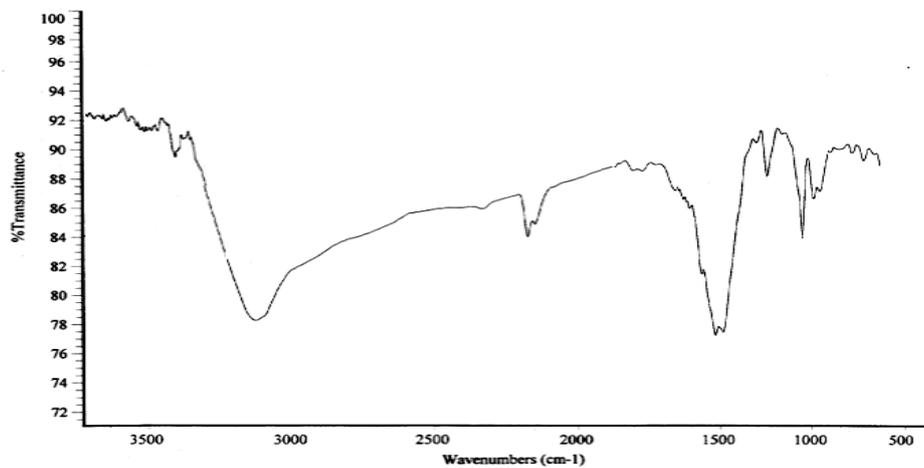
Fig 3: FTIR spectra for BVC (HNO$_3$)
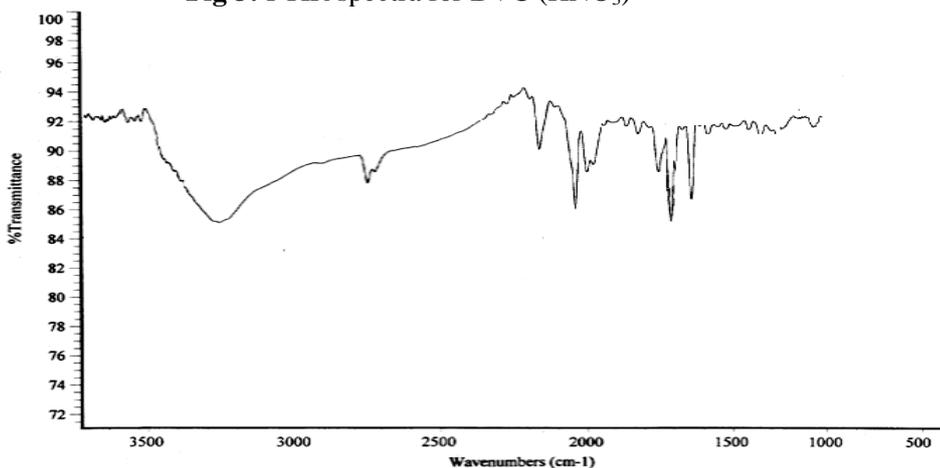
Fig 4: FTIR spectra for BVC (H$_3$PO$_4$)

3.6 Scanning Electron Microscope (SEM)
Scanning electron microscope (SEM - JEOL, JSM 6360 LV) was used to know the surface texture and porosity of the sample (fig 5 & 6). A thin layer of platinum was sputter-coated on the samples for charge dissipation during SEM imaging. The sputter coater (Eiko IB-5 Sputter Coater) was operated in an argon atmosphere using a current of 6mA for 3 min. The coated samples were then transferred to the SEM specimen chamber and observed at an accelerating voltage of 5 kV, eight spot size, four aperture and 15mm working distance.
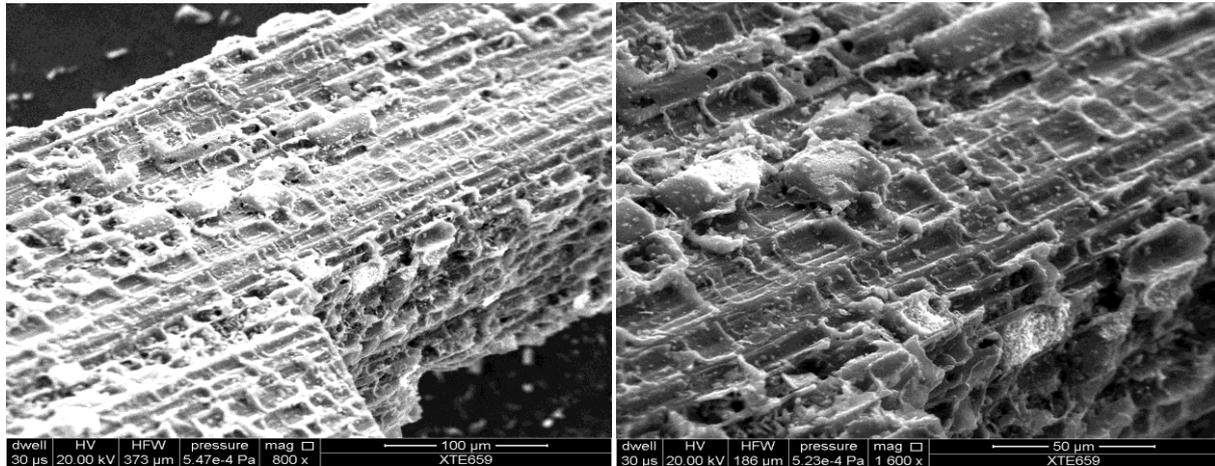
Fig 5: SEM micrograph of BVC (HNO$_3$) at 800 x and 1600 x magnification
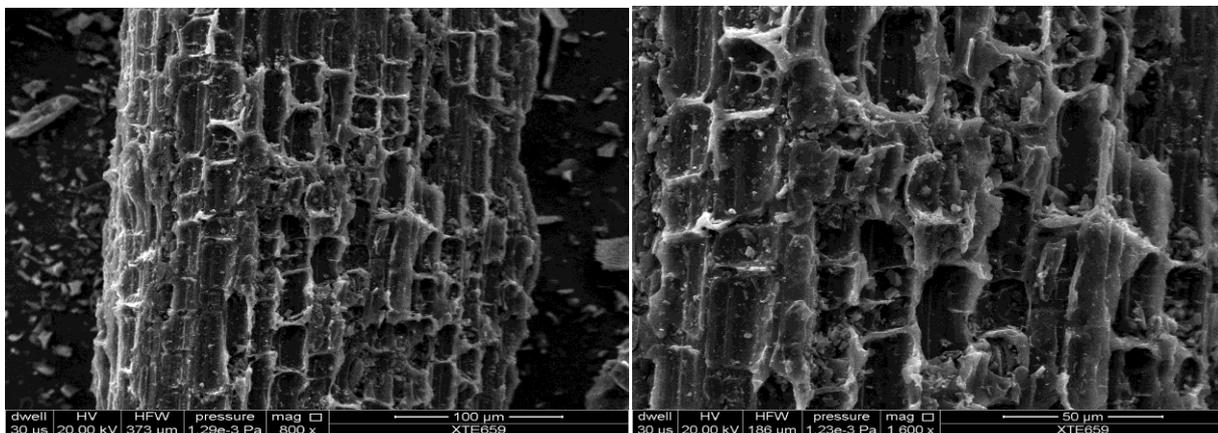
Fig 6: SEM micrograph of BVC (H$_3$PO$_4$) at 800 x and 1600 x magnification

3.7 Energy Dispersive X-ray Analysis (EDX)

Energy Dispersive X-ray Analysis (EDX) technique is used for performing elemental analysis or chemical characterization of a sample in conjunction with Scanning Electron Microscopy (SEM).For determining elemental content, the electron-beam strikes the surface of conducting sample (SEM) .The energy of the beam is typically in the range of 10-20 keV. This causes X-rays to be emitted from the irradiated material. The energy of the X-rays emitted depends on the material under examination. The X-rays are generated in a region about 2 microns in depth. By moving the electron beam across the material a 2-D (two dimensional) image of each element in the sample can be acquired. Due to the low X-ray intensity, images usually take a number of hours to be acquired (fig 7 & 8). Elements of low atomic number are difficult to detect by EDX. Table 5 & 6 shows the elemental composition of the two adsorbents understudy obtained from EDX studies, where the symbol K-ratio is the ratio of the intensity (number of X-ray counts) in the filtered peak for an element of interest in the sample to the intensity in the filtered peak for the standard assigned to that element. Symbol Z stands for the atomic number of the element, symbol A and F are the absorbance and fluorescence values to compensate for the X-ray peak interaction.

Table 5: Elemental composition from EDX of BVC (HNO$_3$)

Element	Weight%	Atomic %	K-Ratio	Z	A	F
C K	87.12	90.14	0.7073	1.0023	0.8099	1.0001
O K	12.56	9.75	0.0166	0.9857	0.1341	1.0000
S K	0.12	0.05	0.0012	0.9233	1.0151	1.0002
Ca K	0.19	0.06	0.0019	0.9144	1.0597	1.0000
Total	100	100				

Table 6: Elemental composition from EDX of BVC (H_3PO_4)

Element	Weight %	Atomic %	K-ratio	Z	A	F
C K	83.75	87.95	0.5410	1.0036	0.6436	1.0001
O K	14.00	11.04	0.0190	0.9869	0.1375	1.0000
Si K	2.24	1.01	0.187	0.9468	0.8834	1.0000
S K	0.01	0.00	0.0001	0.9246	0.9851	1.0000
Ca K	0.00	0.00	0.0000	0.9156	1.0511	1.0000
Total	100	100				
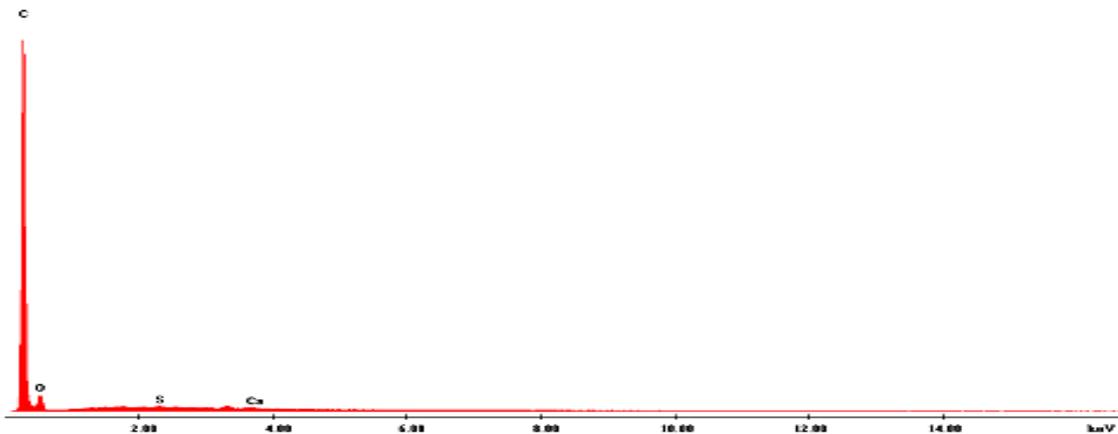
Fig 7: EDX spectra of BVC (HNO_3)
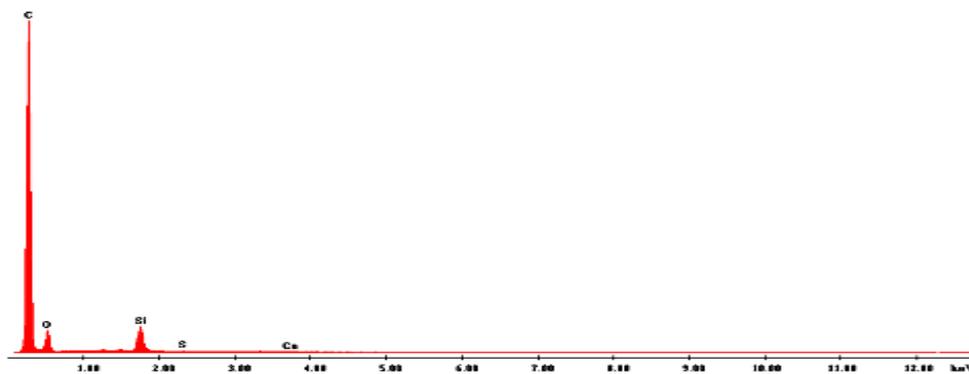
Fig 8: EDX spectra of BVC (H_3PO_4)

4. Adsorption studies

Adsorption isotherm considers a relationship between adsorption capacity and concentration of the remaining adsorbate at constant temperature [21]. Langmuir, Freundlich and Temkin adsorption isotherm models are employed in this study to describe the experimental adsorption isotherm. Langmuir adsorption is based on the fact that maximum adsorption corresponds to a saturated monolayer of solute molecules on the adsorbent surface [22,23]. The linear form of the Langmuir equation can be represented by [24]

$$\text{Percentage removal} = 100 \, \frac{(C_i - C_f)}{C_i} \; ; \; \text{Amount adsorbed} \quad q_e = \frac{(C_i - C_f)V}{M}$$

where C_i and C_f are the initial and final equilibrium solution concentrations of the dye (mg/ L), V is the volume of the solution (L) and M is the mass of the activated carbon (g). The data obtained have been analyzed for adsorption isotherms models.

JMES

4.1 Adsorption Isotherm

Adsorption isotherm considers a relationship between adsorption capacity and concentration of the remaining adsorbate at constant temperature [21]. Langmuir, Freundlich and Temkin adsorption isotherm models are employed in this study to describe the experimental adsorption isotherm. Langmuir adsorption is based on the fact that maximum adsorption corresponds to a saturated monolayer of solute molecules on the adsorbent surface [22,23]. The linear form of the Langmuir equation can be represented by [24]

$$\frac{C_e}{q_e} = \frac{1}{b} Q_0 + \frac{C_e}{Q_0}$$

Where q_e is the amount of methylene blue adsorbed (mg/ g) and C_e is the equilibrium concentration of methylene blue in the bulk solution (mg/ L) while Q_0 is the monolayer adsorption capacity (mg/ g) and b is the Langmuir constant related to energy adsorption capacity. The constants Q_0 and b can be calculated (table 7) from slope and intercept of the plot C_e/q_e vrs C_e [24,25].

Table 7: Effect of initial concentration of methylene blue with different adsorbents

Adsorbent sample	*Initial* conc. [C_i]	Final Conc. [C_e]	Percent removal	Amount adsorbed [q_e]	C_e/q_e	Log C_e	Log q_e
BVC(HNO$_3$)	5	0.0654	98.69	0.4934	0.1325	-1.1844	-0.3068
	10	0.2160	97.84	0.9784	0.2207	-0.6655	-0.0094
	15	0.6914	95.39	1.4308	0.4832	-0.1602	0.1555
	20	1.1160	94.42	1.8884	0.6227	0.0476	0.2760
	25	1.4916	94.03	2.3508	0.7195	0.1736	0.3712
	30	1.6334	94.55	2.8366	0.6463	0.2130	0.4527
	35	1.8810	94.62	3.3119	0.6606	0.2743	0.5200
	40	2.2510	94.37	3.7749	0.6492	0.3523	0.5769
	45	3.1973	92.89	4.1802	0.7648	0.5047	0.6211
BVC(H$_3$PO$_4$)	5	0.0758	98.40	0.4924	0.1539	-1.1203	-0.3076
	10	0.1825	98.17	0.9817	0.1859	-0.7387	-0.0080
	15	0.6012	95.99	1.4398	0.5564	0.2209	0.1583
	20	1.2110	93.94	1.8739	0.6462	0.0831	0.2727
	25	1.6800	93.28	2.3320	0.7204	0.2253	0.3677
	30	2.4000	92.00	2.7600	0.8695	0.3802	0.4409
	35	3.6201	90.88	3.1379	1.0172	0.5040	0.4966
	40	4.0311	89.92	3.5968	1.1207	0.6054	0.5559
	45	4.6210	89.73	4.0379	1.1939	0.6647	0.6061

Freundlich isotherm is an empirical equation describing the heterogeneous adsorption and assumes that different sites with several adsorption energies are involved [25]. The linear form of the Freundlich equation is shown below.

$$\log q_e = \log k + \frac{1}{n} \log C_e$$

$$q_e = \frac{RT}{b_T} \ln (A_T.C_e)$$

The slope 1/n gives adsorption capacity and intercept log K gives adsorption intensity from straight portion of the linear plot obtained by plotting log q_e versus log C_e. Temkin isotherm model predicts a uniform distribution of binding energies over the population of surface binding adsorption [26]. This isotherm assumes that (i) the heat of adsorption of all the molecules in the layer decreases linearly with coverage due to adsorbent-adsorbate interactions, and that (ii) the adsorption is characterized by a uniform distribution of binding energies, up to some maximum binding energy [27]. The Temkin isotherm is applied in the following form [28].
The linear form of Temkin equation is

$$q_e = \frac{RT}{b_T} \ln A_T + \frac{RT}{b_T} \ln C_e$$

$$q_e = \beta \ln\alpha + \beta \ln C_e$$

Where, $\beta = \dfrac{RT}{b_T}$; $\alpha = A_T$

T is the absolute temperature in Kelvin, R is the universal gas constant, 8.314 J/mol K, b_T is the Temkin constant related to heat of sorption (J/mg) and A_T the equilibrium binding constant corresponding to the maximum binding energy (L/g) The Temkin constants A_T and b_T are calculated from the slopes and intercepts of q_e vs $\ln C_e$ (table 8).

Table 8: Adsorption isotherm parameters of the adsorbents

Model	BVC(HNO$_3$)	BVC(H$_3$PO$_4$)
Langmuir isotherm		
Intercept (1/KL)	0.33883	0.32241
Slope (aL/KL)	0.00400	0.00402
Correlation Coefficient		
(r)	0.87861	0.95947
Freundlich isotherm		
Intercept	0.01869	0.02845
Slope (1/n)	0.03617	0.04836
Correlation Coefficient		
(r)	0.72301	0.99834
Temkin isotherm		
b$_T$ (J/mg)	4.0846	3.4348
A$_T$(L/g)	0.19114	0.19004
(r)	0.90751	0.8987
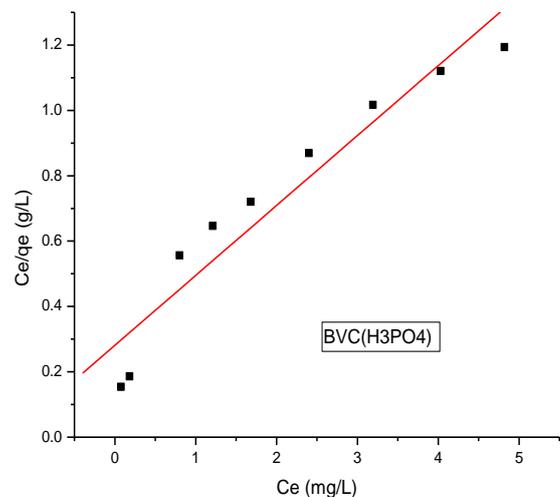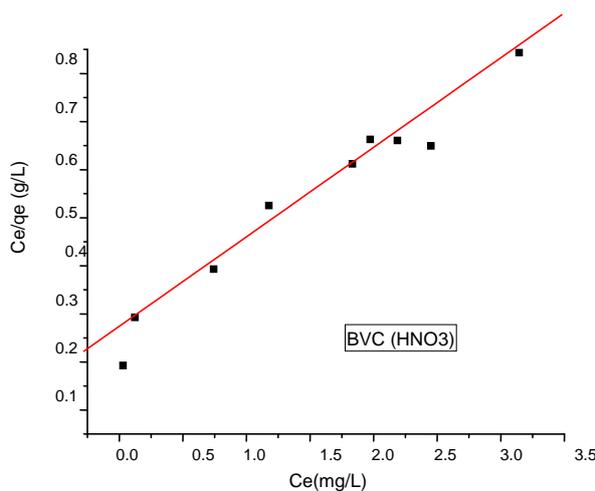
Fig 9: Langmuir adsorption isotherms for the removal methylene blue by different adsorbent

---
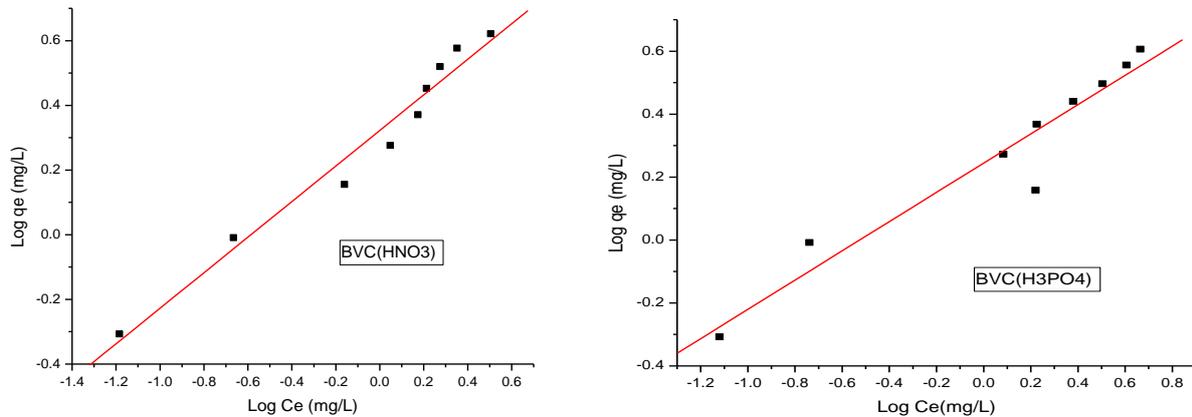
Fig 10: Freundlich adsorption isotherms for the removal of methylene blue by different adsorbents.
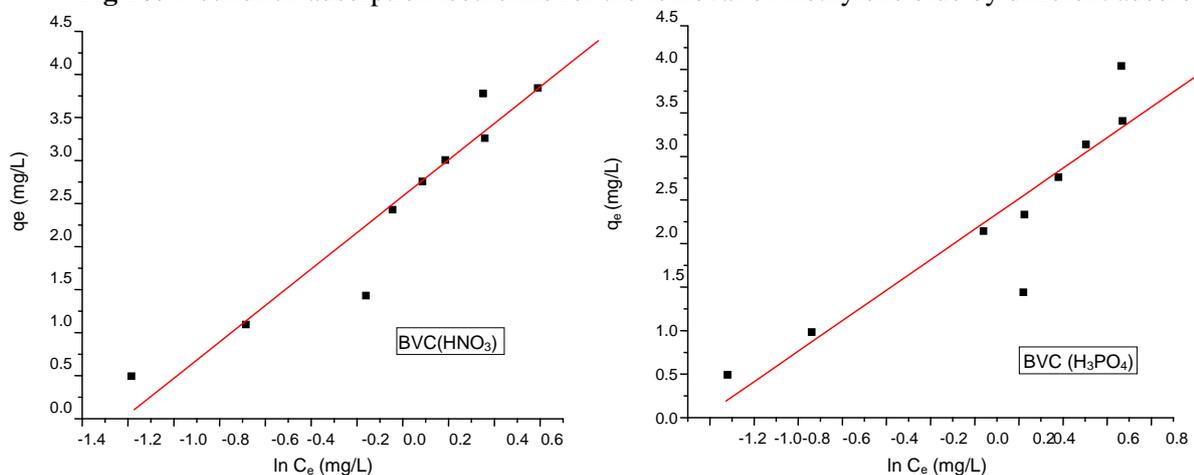
Fig 11: Temkin adsorption isotherms for the removal of methylene blue by different adsorbents.

5. Results and Discussion

The various results obtained from different techniques used for surface characterization of synthesized activated carbon have been discussed as follows.

5.1 Determination of surface area (BET method)

The BET specific surface area of BVC (HNO_3) sample as shown in table.1 shows high surface area of 570 m^2/g which is capable of more monolayer coverage [33] compared to other activated carbons under study. It also gives reasonable values for the average enthalpy of adsorption in the first layer and satisfactory values for V_m, the monolayer capacity of the adsorbate which can be used to calculate the specific surface area of the solid adsorbent [34]. It can be concluded that the surface area of the resulting activated carbons can be designed by varying the amount of the activation agents.

5.2 Zero point charge (pH ZPC)

The pH at zero point charge in all the cases is above 7.0 (fig.1 and fig.2). The results form table. 1 and table.2 show that pH < pH $_{zpc}$ indicating the surface is positively charged which arises from the basic sites that combine with protons from the medium [17].

5.3 Iodine number

The iodine number is a relative indicator of porosity in an activated carbon. The results form table.3 for iodine number of the two different carbons activated with HNO_3 and H_3PO_4 shows a higher value of iodine number from HNO_3 activation in comparison to H_3PO_4 activation which may due to higher degree of activation which enables more adsorption of iodine molecule.

5.4 Boehm titration method

Surface functional group determined by Boehm titration method as indicated in table.3 clearly indicates that the total basic groups are slightly greater than the total acid groups. The basicity may be due to oxygen functional group which characterizes the amount of surface basic group's that are present in the activated carbon [19].

5.5 FT-IR (Fourier Transform Infrared Spectroscopy)

The results for FT-IR of the two different carbons activated with HNO_3 and H_3PO_4 are presented in Table 4. The IR-bands from fig.3 and fig.4 for BVC (HNO_3) and BVC (H_3PO_4) shows a broad peak at 3215-3125 cm^{-1} which is due to the absorption of water molecules as result of an O-H stretching mode of hydroxyl groups and adsorbed water. The band of asymmetric at lower wave numbers indicates the presence of strong hydrogen bonds [29, 30]. Bands at 2714 cm^{-1} shown by BVC (H_3PO_4) are connected with $(C-H)_s$ and $vs(C-H)_{as}$ vibrations (s=symmetric, as=asymmetric).The C=O vibration near 1821-1642 cm^{-1} (fig.4) is the specific peak for the carboxylic acid, aldehydes, ketones, esters and lactones groups. The v(C=C) vibration mode at about 1510 cm^{-1} (fig.3) are probably due to stretching vibration of C=O moieties of conjugated systems or aromatic ring stretching coupled to highly conjugated carbonyl groups[31]. While the bands at 1245, and1125 cm^{-1} are clearly observed and correspond to C-O stretching bonds in phenols, ethers, lactones. Bands at 1062,and 1068 cm^{-1} correspond to alcoholics C-O stretching vibration [32].The formation of C-O stretching of oxygenated groups may be attributed to redox reactions of incorporated HNO_3 and H_3PO_4 with carbon during the chemical treatment [33]. The band at wave number below 874 cm^{-1} may be related to out of the plane bending modes.

5.6 Scanning Electron Microscope (SEM)

The micrographs (fig.5 and fig.6) from SEM analysis of the activated carbons show a highly developed pore structure for both the adsorbents. It is evident that there are larger numbers of pores present in the activated carbon produced using Nitric acid (HNO_3) activation than the activated carbon obtained from phosphoric acid (H_3PO_4).

5.7 Energy Dispersive X-ray Analysis (EDX)

EDX graphs from fig. 7 and fig.8 show that the carbon samples primarily consist of carbon and oxygen at varied proportions. The carbon and oxygen content is higher in BVC (HNO_3) and less in BVC (H_3PO_4). EDX analysis of the samples (table.5 and table.6) practically does not show the presence of Nitrogen; neither does it show Phosphorus which could explain the rather good adsorbent properties observed particularly for this activated carbon.

5.8 Adsorption studies

Three models of adsorption isotherm namely Langmuir, Frendulich and Temkin were applied for the adsorbents under study, and the results (table.8) obtained gave a high correlation value in the range of 0.72301-0.99834. So, these activated carbons can be effectively used for the removal of methylene blue dye. However among the three models, Temkin model from fig.11 showed almost linearity among the adsorption points in the straight line equation as compared to Langmuir model (fig.9) and Frendulich model (fig.10), thus Temkin model showed a higher coefficient correlation value of 0.8987 - 0.94864 which indicates that the heat of adsorption of all the molecules in a layer decreases linearly due to adsorbent-adsorbate interactions.

Conclusion

Activated carbon was prepared from stem and leaves of *Bambusa vulgaris (BVC)*, for which thermal treatment subsequently followed by chemical activation using different acids were done. The principle behind the chemical activation of activated carbon was to introduce certain functional groups on the surface of the carbon in order to enhance the adsorption capacity. Various experiments like iodine number, Boehm titration, methylene blue adsorption, pHpzc, FTIR, SEM, EDX and BET method have been done to compare the effectiveness and adsorption capacity between the two activated carbons understudy. Both the adsorbents showed properties like high iodine number, high fixed carbon value which contributes to the increase in the adsorption ability. The statement is well supported by the SEM/EDX data. The adsorbents BVC (HNO_3) has the better adsorption characters due to high surface area of 570 m^2/g as compared to 530 m^2/g for BVC (H_3PO_4), this is well supported by the SEM/EDX data. The SEM micrographs also suggest BVC (HNO_3) has greater

number of pores than other adsorbents under study. EDX studies further strengthen the fact that BVC (HNO_3) is the better activated carbon produced with the higher carbon content and the less oxygen content. Thus it may be concluded that the chemical structure of the activated carbon were found to be influenced markedly with its activation scheme and thus chemical activation by nitric acid is far more better than phosphoric acid. Out of three isotherm models studied Temkin model shows best fit with a correlation coefficient of 0.8987 - 0.94864, this indicates that the fall in the heat of adsorption is linear and the free energy of sorption is a function of the surface coverage. Thus the prepared activated carbons are being successfully used for the removal of organic dyes like methylene blue from aqueous phase as adsorption as it is evident from the results.

References

1. Tang S., Zhu Z.H. *Dyes and Pigments*, 75 (2007) 306–314.
2. Bhatnagar Amit., Hogland William., Marques Marcia, Sillanpaa Mika, *Chem. Eng. J.,* 219 (2013) 499-511.
3. Utrilla Rivera., Sánchez-Polo M., Gómez-Serrano V., Álvarez P. M., Alvim-Ferraz M.C.M., Dias J.M. *J. Hazard. Mater.* 187 (2011) 1-23.
4. Gamal O., El-Sayed,Mohamed M., Yehia, Amany A., Asaad. *Water Res. Industry***,** 7–8 (2014) 66–75.
5. Budinova T., Ekinci E., Yardim F., Grimm A. Björnbom E., Minkova V., Goranova M., *Fuel Procs. Techn.* 87 (2006) 899–905.
6. Teresa, Bandosz J. Activated carbon surfaces in environmental remediation, Elsevier, (2006).
7. Onal Y., Akmil-Basar C., Sarıcı-Ozdemir C., Erdogan S., *J. Hazard. Mater.* 142 (2007)138–143.
8. Nhapi I., Banadda N., Murenzi R., Sekomo C.B., Wali U.G., *The Open Environ. Eng. J.* 4 (2011*)*170-180**.**
9. Hameed B.H., Din A.T.M., Ahmad A.L., *J. Hazard. Mater.* 141 (2007) 819–825.
10. Hameed B.H., Ahmad A.L., Latiff K.N.A. *Dyes Pigments.* 75 (2007) 143–149.
11. Legrouri K., Khouya E., Ezzine M., Hannache H., Denoyel R., Pallier R., Naslain R., *J. Hazard. Mater.* 118 (2005) 259–263.
12. Prakash Kumar B.G., Shivakamy K., Lima Rose Miranda., Velan M. *J. Haz. Mater.* 136 (2006) 922-929
13. Tan I.A.W., Hameed B.H., Ahmad A.L. *Chem. Eng. J.* 127(2007) 111–119.
14. Basar C.A. *J. Hazard. Mater.* 135(2006) 232–241.
15. Tan I.A.W., Hameed B.H., Ahmad A.L. *Chem. Eng. J.* 137(2008)462–470 .
16. Kosmulski M., *J.Colloid Interface Sci.* 253 (2002) 77-87.
17. Kosmulski M., *J. Colloid and Interface Sci.* 337 (2009) 439–448.
18. Annual Book of ASTM Standards , Philadelphia PA, United State of America. (2006).
19. Boehm H.P., *Carbon.* 32-5 (1995) 759-769.
20. Boehm H. P.*, Carbon.* 40- 2 (2002)145-149.
21. Patnukao P., Kongsuwan A., Pavasant P. *J. Environ. Sci.* 20 (2008) 1028–1034.
22. Arica M.Y., Bayramoglu .G., Yılmaz M., Genc O., Bektas S. *J Hazard Mater.* 109(2004)191–199.
23. Sheng PX., Ting YP., Chen JP., Hong L . *J Colloid Interface Sci* .27 (2004) 131–141.
24. Bouhamed F., Elouear Z., Bouzid J. *J. of the Taiwan Inst. of Chemical Eng.* 43(2012) 741-749.
25. Rengaraj S., Joo C.K., Kim Y., Yi J. *J. Hazard. Mater.* B 102 (2003) 257-275.
26. Temkin M.J., Pyzhev V. *Acta Physiochim.* 12 (1940) 217– 222.
27. Gouamida M., Ouahrania M.R., Bensaci M.B. *Energy Procedia.*36 (2013) 898 – 907.
28. Areco M.M., Afonso M.S. *Biointerfaces* .81 (2010) 620–628.
29. R.A. and Carlson, G.L. *Fuel.* 51 (1972) 194-198.
30. Coleman P.B. Practical Sampling Techniques for Infrared Analysis, CRC Press, (1993).
31. Smith B. Infrared Spectral Interpretation, a Systematic Approach, CRC Press, (1999).
32. Coates J.P. *Appl. Spectrosc. Rev.* 31(1–2) (1996) 179–192.
33. Harry Marsh., Franciso Rodriguez-Reinoso. Activated carbon, Elsevier science & Technology books, **ISBN**-13: 9780080444635 (2006).

(2017) ; http://www.jmaterenvironsci.com